

Mapping repulsive to attractive interaction in driven-dissipative quantum systems

Andy C. Y. Li and Jens Koch

Department of Physics and Astronomy, Northwestern University, Evanston, Illinois 60208, USA

(Dated: April 28, 2022)

Repulsive and attractive interactions usually lead to very different physics. Striking exceptions exist in the dynamics of driven-dissipative quantum systems. For the example of a photonic Bose-Hubbard dimer, we establish a one-to-one mapping relating the cases of onsite repulsion and attraction. We prove that the mapping is valid for an entire class of Markovian open quantum systems with time-reversal invariant Hamiltonian and physically meaningful inverse-sign Hamiltonian. To underline the broad applicability of the mapping, we illustrate the one-to-one correspondence between the nonequilibrium dynamics in a geometrically frustrated spin lattice and that in a non-frustrated partner lattice.

I. INTRODUCTION

Photonic quantum systems provide a versatile platform to study nonequilibrium many-body phenomena of light [1–5], dissipative phase transitions [6–11], and dissipation engineering [12–17]. The nonequilibrium dynamics and steady-state properties of driven-dissipative systems also play a crucial role in the development of quantum information technology for quantum optimal control and open-system state stabilization [14, 17–19]. Despite the immense theoretical and experimental progress in this field, understanding the dynamics at an intuitive level often remains challenging. Considerations based on energetically favorable states are not generally appropriate in nonequilibrium, and can in fact be misleading.

We show that this is, in particular, the case for a driven-dissipative Bose-Hubbard dimer. Specifically, suppose that bosonic excitations are fed coherently into a dimer site, where they are subject to hopping, onsite interaction, and dissipation. How will the physics change when the sign of the onsite interaction is swapped, so that onsite repulsion turns into onsite attraction? In this paper, we demonstrate that there is an exact mapping relating observable expectation values for the repulsive system to those of the attractive system. In other words, while the equilibrium physics of a Bose-Hubbard dimer with conserved particle number is extremely different for attraction vs. repulsion [20], we find that the nonequilibrium dynamics of a driven-dissipative Bose-Hubbard dimer essentially does not distinguish between the repulsive and attractive case.

The mapping can be generalized and holds for a large class of Markovian open quantum systems with time-reversal invariant system Hamiltonian. It relates the nonequilibrium dynamics of an open system Q_1 , associated with Hamiltonian H , to that of another system Q_2 , associated with the negative-partner Hamiltonian $-H$. As long as $-H$ has physical meaning (e.g., as an effective Hamiltonian in a rotating frame), the mapping guarantees a one-to-one correspondence between observable expectation values in two different quantum systems Q_1 and Q_2 .

In the remainder of this paper, we first discuss the Bose-Hubbard dimer model with drive and dissipation, approaching the mapping from the point of view of the equations of motion for system observables. We then prove that the result is an instance of the more general mapping, namely the Hamiltonian sign inversion (HSI) mapping, which is applicable to a broad range of driven-dissipative systems. We illustrate this point by the discussion of another example, namely the mapping of the spin dynamics in a geometrically frustrated lattice to corresponding dynamics in a non-frustrated spin lattice.

II. DRIVEN-DISSIPATIVE BOSE-HUBBARD DIMER: MAPPING POSITIVE TO NEGATIVE U

We consider a driven-dissipative Bose-Hubbard dimer [21–24] with either repulsive or attractive onsite interaction, $U > 0$ or $U < 0$, respectively. By inspection of the equations of motion, we will reveal an exact mapping between the cases of positive and negative U , i.e., between dimers with repulsive and attractive onsite interaction. The notion of such a mapping may, at first, seem to contradict the common intuition that attraction and repulsion must lead to entirely different physics. In our following derivation of the HSI mapping for the driven-dissipative Bose-Hubbard dimer, we will carefully discuss how this contradiction is resolved, and what exactly the mapping does and does not imply.

In concrete terms, the Bose-Hubbard dimer is described by the Hamiltonian

$$H_{\pm} = \sum_{n=1}^2 (\omega a_n^{\dagger} a_n + U_{\pm} a_n^{\dagger} a_n^{\dagger} a_n a_n) + J (a_1^{\dagger} a_2 + a_2^{\dagger} a_1), \quad (1)$$

and consists of two sites, $n = 1, 2$, with onsite energy ω (we set $\hbar = 1$ throughout) and Hubbard interaction of strength $U_{\pm} \geq 0$. Equation (1) captures both the repulsive case (positive U) via H_+ , and the attractive case (negative U) via H_- . Bosonic excitations are created by \mathbf{a}_n^\dagger and can hop between the two sites $n = 1, 2$ with rate J .

Simple energetic considerations suggest that repulsion and attraction lead to rather different results: In the positive- U dimer, bosons repel: the onsite interaction $U_+ \mathbf{a}_n^\dagger \mathbf{a}_n^\dagger \mathbf{a}_n \mathbf{a}_n$ increases the energy quadratically with the number of bosons on each site. For fixed boson number $N \gg 1$, the onsite interaction is minimized by dividing the boson number equally between the two sites. By contrast, in the negative- U dimer, bosons attract: the Hubbard term $U_- \mathbf{a}_n^\dagger \mathbf{a}_n^\dagger \mathbf{a}_n \mathbf{a}_n$ lowers the energy quadratically with the number of bosons on each site. For fixed boson number $N \gg 1$, the onsite energy can thus be minimized by having all bosons occupy the same site. (We note that the spectrum of H_- is not bounded from below if the boson number is not fixed: ultimately, adding more and more bosons will lower the energy indefinitely. In practice, the attractive Bose-Hubbard dimer may serve as an *effective* model, in which additional nonlinear interactions need to be included when the boson number exceeds a certain threshold. Such additional terms restoring boundedness of the spectrum will naturally be system dependent [39].)

The above considerations yield the correct picture describing the ground-state physics for a closed-system Bose-Hubbard dimer. However, different physics becomes important for an *open-system* dimer, in which bosons are not understood as massive particles but rather as excitations that can be created by a coherent drive, as well as disappear from the system by energy dissipation. Concrete examples of such a system are coupled nonlinear resonators in which photons are the bosonic excitations in question [3, 10, 11]. The HSI mapping we wish to derive becomes meaningful in this open-system setting, where it relates the nonequilibrium dynamics of the positive- U dimer to that of the negative- U dimer.

For our derivation, we assume weak system-bath coupling and validity of the Markov approximation, so that we can describe the time evolution and steady state of the open Bose-Hubbard dimer within the Lindblad master equation formalism [25, 26]. The reduced density matrices ρ_{\pm} for positive or negative U then evolve according to

$$\frac{d\rho_{\pm}}{dt} = -i[H_{\pm}, \rho_{\pm}] + \gamma \sum_{n=1}^2 \mathbb{D}[\mathbf{a}_n] \rho_{\pm}, \quad (2)$$

where $\mathbb{D}[\mathbf{a}_n]\rho \equiv \mathbf{a}_n \rho \mathbf{a}_n^\dagger - \frac{1}{2} \mathbf{a}_n^\dagger \mathbf{a}_n \rho - \frac{1}{2} \rho \mathbf{a}_n^\dagger \mathbf{a}_n$ is the dissipator describing the non-unitary evolution induced by the system-bath coupling. The jump operators \mathbf{a}_n produce bosonic excitation loss from each site, as is appropriate, e.g., to describe intrinsic photon loss in transmission-line resonators or optical cavities. We remark that Eq. (2) is widely used to describe the open Bose-Hubbard dimer and related models even though, strictly speaking, the employed jump operators do not obey the requirement that jump operators be operators projecting from one eigenstate of the Hamiltonian to another one [25]. It is worth noting that use of such ‘‘phenomenological’’ dissipators has yielded quantitative agreement with experimental data for driven-dissipative photonic systems in specific parameter regimes [3, 10, 11, 27]. A more detailed discussion of this point is beyond the scope of this paper.

While both H_+ and H_- conserve the total number of bosonic excitations, dissipation induces relaxation of the dimer towards its vacuum state. An external drive can establish a balance between excitation loss and gain. For concreteness, we consider a coherent tone driving the first dimer site as described by the drive Hamiltonian $H_d(t) = \epsilon(\mathbf{a}_1^\dagger e^{-i\omega_d t} + \text{h.c.})$. Here, ϵ parametrizes the strength of the drive, and ω_d its frequency. In the frame co-rotating with the drive, the effective system Hamiltonian is time independent,

$$H_{\pm}^{\text{eff}} = \sum_{n=1}^2 [\delta\omega \mathbf{a}_n^\dagger \mathbf{a}_n + U_{\pm} \mathbf{a}_n^\dagger \mathbf{a}_n^\dagger \mathbf{a}_n \mathbf{a}_n] + \epsilon(\mathbf{a}_1^\dagger + \mathbf{a}_1) + J(\mathbf{a}_1^\dagger \mathbf{a}_2 + \mathbf{a}_2^\dagger \mathbf{a}_1), \quad (3)$$

where $\delta\omega \equiv \omega - \omega_d$ denotes the detuning between resonator and drive frequency.

We demonstrate the HSI mapping at the level of expectation values. Consider for instance $\langle \mathbf{a}_1 \rangle$, whose real and imaginary parts yield the two field quadratures I and Q in quantum-optics language. For positive- U and negative- U interaction, respectively, the time evolution of $\langle \mathbf{a}_1 \rangle$ is governed by

$$i \frac{d\langle \mathbf{a}_1 \rangle_+}{dt} = \left(\delta\omega - \frac{i\gamma}{2} \right) \langle \mathbf{a}_1 \rangle_+ + 2U_+ \langle \mathbf{a}_1^\dagger \mathbf{a}_1^2 \rangle_+ + J \langle \mathbf{a}_2 \rangle_+ + \epsilon, \quad (4)$$

$$i \frac{d\langle \mathbf{a}_1 \rangle_-}{dt} = \left(\delta\omega - \frac{i\gamma}{2} \right) \langle \mathbf{a}_1 \rangle_- + 2U_- \langle \mathbf{a}_1^\dagger \mathbf{a}_1^2 \rangle_- + J \langle \mathbf{a}_2 \rangle_- + \epsilon. \quad (5)$$

Our claim, to be substantiated in the following, is that the dynamics for negative- U interaction can be obtained exactly from the dynamics for positive- U interaction. To make this argument, we now consider the positive- U system. For convenience, we introduce the notation $\langle \mathbf{a}_1(\mathbf{p}) \rangle_+$, where $\mathbf{p} = (U_+, \delta\omega, \epsilon, J)$ collects all external parameters entering

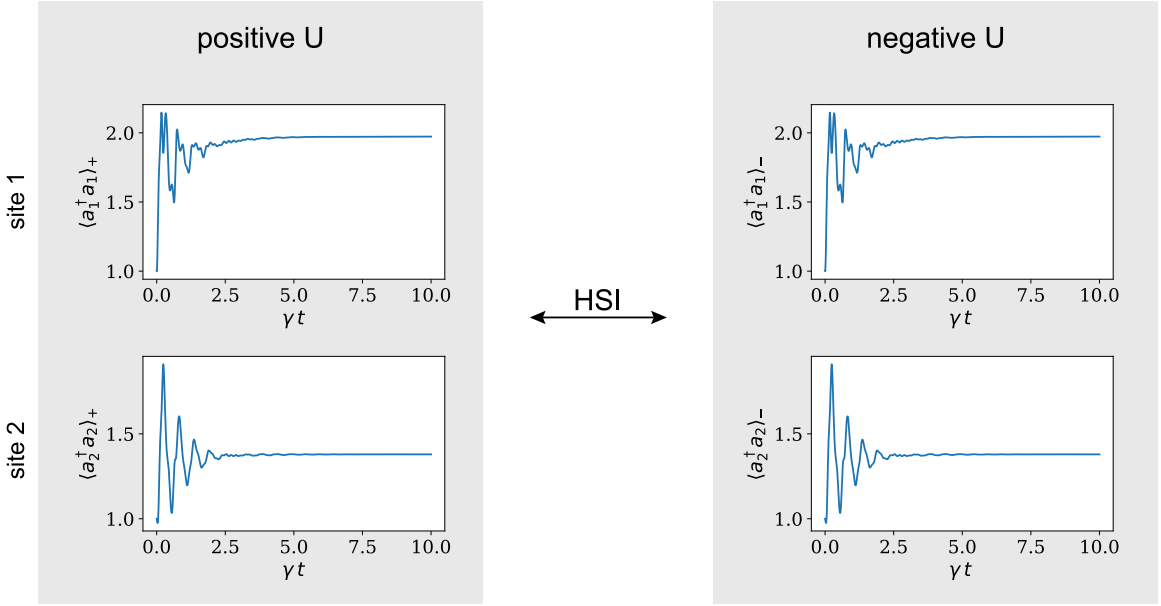


FIG. 1: **Excitation numbers on the two sites of a repulsive and attractive Bose-Hubbard dimer.** The excitation numbers $\langle a_1^\dagger a_1 \rangle_\pm$ and $\langle a_2^\dagger a_2 \rangle_\pm$ are observed to follow the same dynamics in the repulsive (+) and and attractive case (-). For both dimer models, the $t = 0$ initial state is the Fock state with one excitation on each site. (Parameters: $\delta\omega/\gamma = \pm 1$, $U/\gamma = \pm 5$, $\epsilon/\gamma = 15$ and $J/\gamma = 10$.)

the Hamiltonian H_+^{eff} [Eq. (3)]. (Note that we purposely do *not* include the dissipation rate γ in \mathbf{p} .) Next, we take the complex conjugate of Eq. (4) and write it in the form

$$i \frac{d\langle a_1(\mathbf{p}) \rangle_+^*}{dt} = \left(-\delta\omega - \frac{i\gamma}{2} \right) \langle a_1(\mathbf{p}) \rangle_+^* + 2U_- \langle a_1^\dagger a_1^2(\mathbf{p}) \rangle_+^* - J \langle a_2(\mathbf{p}) \rangle_+^* - \epsilon, \quad (6)$$

where we have used that $-U_+ = U_-$. Comparison with Eq. (5) is suggestive of the relation

$$\langle a_1(-\mathbf{p}) \rangle_- = \langle a_1(\mathbf{p}) \rangle_+^*, \quad (7)$$

i.e., expectation values for the cases of attractive and repulsive onsite interaction are the same up to complex conjugation and sign adjustments of remaining Hamiltonian parameters. However, a firm proof of this relation requires that analogous relations also hold for $\langle a_2 \rangle_+^*$ and $\langle a_1^\dagger a_1^2 \rangle_+^*$ and thus, due to the ensuing hierarchy of equations of motion, for all expectation values $\langle A_{r,s}^{p,q} \rangle_+^* = \langle (a_1^\dagger)^p (a_2^\dagger)^q a_1^r a_2^s \rangle_+^*$. We show in Appendix A that the relation (7) indeed carries over to the general case:

$$\langle A_{r,s}^{p,q}(-\mathbf{p}) \rangle_- = \langle A_{r,s}^{p,q}(\mathbf{p}) \rangle_+^*. \quad (8)$$

In simple words: every expectation value describing the dynamics for negative- U interaction can be obtained from a corresponding expectation value for positive- U interaction by the following two steps. First, invert the sign of each Hamiltonian parameter, while leaving the signs of decoherence rates unchanged. Second, replace expectation values by their complex conjugates. The relation Eq. (8) therefore establishes a one-to-one map between positive- U and negative- U interaction through Hamiltonian sign inversion. This is summarized by the diagram

$$\begin{array}{ccc}
 Q_1 & \begin{array}{l} \text{system parameters } U_+ > 0; \delta\omega, J, \epsilon \\ \text{damping rate } \gamma \\ \text{expectation values } \langle A \rangle_1 \end{array} & \xleftrightarrow{\text{HSI}} \\
 & & \begin{array}{l} Q_2 \\ \text{system parameters } U_- = -U_+; -\delta\omega, -J, -\epsilon \\ \text{damping rate } \gamma \\ \text{expectation values } \langle A \rangle_2 = \langle A \rangle_1^* \end{array} \\
 & & (9)
 \end{array}$$

where entries in each row specify corresponding Hamiltonian parameters, damping parameters, and expectation values.

In order to make the systems Q_1 and Q_2 with positive and negative U match even more closely, we may eliminate the sign changes in hopping J and drive strength ϵ with a gauge transformation, $\mathbf{a}_1 \rightarrow -\mathbf{a}_1$. At this point, we find

that the dynamics of the attractive versus the repulsive driven-damped Bose-Hubbard dimer is exactly the same when switching from red-detuned to blue-detuned drive frequency, $\delta\omega \rightarrow -\delta\omega$. (A similar observation for a driven-damped nonlinear oscillator was made by Dykman in Ref. 28.) While the ground-state physics of the closed system crucially depends on the sign of the interaction, the nonequilibrium dynamics is identical in the discussed sense. We have confirmed this statement with multiple numerical simulations. An example of simulation results is depicted in Fig. 1. Here, both positive and negative U dimers are initialized in a Fock state with one excitation on each site. The dynamics observed for the excitation numbers on the two sites are found to be identical for positive and negative U . We have confirmed independently that dynamics with different initial states converge to the same steady state for positive and negative U .

It is interesting to note that the HSI mapping enables one to extend previous results for the driven-dissipative Bose-Hubbard dimer to the regime with the opposite sign of interaction. For instance for repulsive interaction, it has been predicted that the steady state of the dimer can undergo spatial symmetry breaking [22]. The HSI mapping, then, implies that the same symmetry breaking must also be present in the attractive dimer model. Surprisingly, the nature of the interaction appears to play only a secondary role in producing the spatial symmetry breaking.

III. HAMILTONIAN SIGN INVERSION MAPPING

In order to prove the HSI mapping that links positive- U and negative- U Bose-Hubbard dimers, we invoked the entire hierarchy of coupled equations of motion for system observables. This approach is cumbersome, and leaves one with the question whether the HSI mapping relies upon specific properties of the Bose-Hubbard dimer, which would limit its scope to this one particular model. We will demonstrate that this is not the case and show that, rather, the HSI mapping generalizes to arbitrary Markovian open quantum systems with time-reversal invariant system Hamiltonians H . (Note that while H may be time-reversal invariant, the coupling of the system to its environment will naturally break overall time-reversal symmetry.) The HSI mapping establishes a one-to-one correspondence between the dynamics of an open quantum system Q_1 with system Hamiltonian H and the dynamics of a partner system Q_2 with system Hamiltonian $-H$. We will base our discussion on the Lindblad master equation, and show that the HSI mapping can be formulated in a straightforward way that entirely bypasses cumbersome considerations of the hierarchy of equations of motion.

The dynamics of the open system Q_1 is governed by the Lindblad master equation [25, 26],

$$\frac{d}{dt}\rho(t) = -i[H, \rho(t)] + \sum_j \gamma_j \mathbb{D}[c_j]\rho(t), \quad (10)$$

which describes the time evolution $t \mapsto \rho(t)$ of the reduced density matrix of Q_1 . The dissipation and dephasing processes from coupling to the environment are encoded by rates γ_j and corresponding jump operators c_j . In the absence of coupling to the environment, the system is assumed to be time-reversal symmetric. As usual, we formalize this symmetry by utilizing the antiunitary time-reversal operator T [29, 30], which must be constructed for each concrete system of interest so that relevant observables obey the appropriate transformation laws, such as $TxT^\dagger = x$ and $TpT^\dagger = -p$ for generalized position and conjugate momentum operators x and p . Time-reversal symmetry of the isolated system then amounts to the identity $THT^\dagger = H$.

We construct the general HSI mapping by considering the T -transform of the density matrix,

$$\rho_T = T\rho T^\dagger. \quad (11)$$

We stress that the evolution $t \mapsto \rho_T(t)$ does *not* correspond to backward-in-time evolution of $t \mapsto \rho(t)$. We obtain the equation of motion for $\rho_T(t)$ by sandwiching Eq. (10) with T and T^\dagger , exploiting that the time-reversal operator obeys $T^\dagger T = \mathbb{1}$, and invoking time-reversal symmetry of the system Hamiltonian. This yields the equation

$$\frac{d}{dt}\rho_T(t) = -i[-H, \rho_T(t)] + \sum_j \gamma_j \mathbb{D}[Tc_j T^\dagger]\rho_T(t). \quad (12)$$

which we recognize as having the proper form of a Lindblad master equation. Hence, we may interpret ρ_T as the density matrix of an open quantum system Q_2 . Comparing this Eq. (12) with the original master equation (10) for ρ , we see that Q_2 has a Hamiltonian with inverted sign, as well as jump operators $Tc_j T^\dagger$.

We can now relate expectation values $\langle A \rangle_2 = \text{Tr}(A\rho_T)$ for system Q_2 back to expectation values for Q_1 . To do so, write $\langle A \rangle_2 = \text{Tr}(TT^\dagger A T\rho T^\dagger)$, but note that the cyclic property of the trace does *not* hold for anti-linear operators such as T . Instead, we simplify the expression further by considering an orthonormal Hilbert space basis of time-reversal

invariant states $\{|n\rangle\}$. In this basis, the action of the time-reversal operator reduces to complex conjugation, such that $\mathbb{T} \sum_n \alpha_n |n\rangle = \mathcal{K} \sum_n \alpha_n |n\rangle = \sum_n \alpha_n^* |n\rangle$. With this, we find

$$\langle A \rangle_2 = \text{Tr}(\mathbb{T} \bar{A} \rho \mathbb{T}^\dagger) = \sum_n \langle n | \mathcal{K} \bar{A} \rho \mathcal{K} | n \rangle = \sum_{m,n} \langle n | \mathcal{K} \langle m | \bar{A} \rho | n \rangle | m \rangle = \text{Tr}(\mathbb{T}^\dagger A \mathbb{T} \rho)^*, \quad (13)$$

where we have temporarily used the shorthand $\bar{A} = \mathbb{T}^\dagger A \mathbb{T}$. As a result, the correspondence between expectation values in system Q_1 and Q_2 takes the form

$$\langle A \rangle_2 = \text{Tr}(A \rho_T) = \text{Tr}(\mathbb{T}^\dagger A \mathbb{T} \rho)^* = \langle \mathbb{T}^\dagger A \mathbb{T} \rangle_1^*. \quad (14)$$

We can summarize the general HSI mapping with the diagram

Q_1	system Hamiltonian H damping rates, ops. γ_j, c_j density matrix $\rho_1(t)$ expectation values $\langle A \rangle_1$	\longleftrightarrow (HSI)	Q_2	system Hamiltonian $-H$ damping rates, ops. $\gamma_j, \mathbb{T} c_j \mathbb{T}^\dagger$ density matrix $\rho_2(t) = \mathbb{T} \rho_1(t) \mathbb{T}^\dagger$ expectation values $\langle A \rangle_2 = \langle \mathbb{T}^\dagger A \mathbb{T} \rangle_1^*$
-------	---	--------------------------------	-------	--

(15)

It is easy to verify that the mapping (9) for the driven-dissipative Bose-Hubbard dimer is a special case of (15). To see this note that: the inversion of the Hamiltonian sign produces the sign changes of system parameters as recorded in Eq. (9); the jump operators considered in the dimer model are time-reversal invariant, $\mathbb{T} a_j \mathbb{T}^\dagger = a_j$ [40], and so are the expectation values of the observables $A_{r,s}^{p,q}$. We note that the general HSI mapping immediately extends the correspondence between positive and negative U dimers to Bose-Hubbard lattices of arbitrary size and lattice geometry.

The HSI mapping is mathematically rigorous, but one must check that the partner system Q_2 is indeed a physically meaningful quantum system. Two aspects are crucial here. First, in infinite-dimensional Hilbert spaces, sign-inversion of the Hamiltonian leads to energy spectra not bounded from below. As shown in the dimer example, this is unproblematic if the Hamiltonian is an effective Hamiltonian in a rotating frame, whose eigenvalues only carry the meaning of quasienergies. Second, the HSI mapping may modify the jump operators entering the master equation.

A wide range of driven open quantum systems is amenable to the HSI mapping, including circuit-QED and ultracold-atoms systems which are of interest in studies of phase transitions [6, 8–11] and quantum state preparation [14, 16–18]. For open quantum systems with finite-dimensional Hilbert space, $-H$ is always physical. This class of system covers a number of quantum systems currently being researched, e.g. open spin lattices [6, 31–34] for which we will present one example in the following section. Here, again, the HSI mapping will link two physically different systems and establish a useful one-to-one correspondence between their nonequilibrium dynamics.

IV. DRIVEN-DISSIPATIVE SPIN LATTICE

The HSI mapping can easily be applied to driven-dissipative (pseudo-)spin lattices which can be realized, for example, by ultracold atoms [34] and circuit-QED devices [35, 36]. We illustrate such an application next, considering an Ising system with one spin per lattice site, each with (Zeeman-)energy splitting Ω . Each spin is driven by a coherent tone with drive strength ϵ_j and frequency ω_d , and is σ^z -coupled to its nearest neighbors with a coupling strength J . The effects of the environment are modeled by spin relaxation with a rate Γ . In the frame co-rotating with the drive, the system dynamics is governed by the master equation

$$\frac{d\rho}{dt} = -i[H, \rho] + \Gamma \sum_{j=1}^N \mathbb{D}[\sigma_j^-] \rho, \quad (16)$$

with system Hamiltonian

$$H_\pm = \sum_{j=1}^N [\delta\Omega \sigma_j^\pm \sigma_j^- + \epsilon_j (\sigma_j^- + \sigma_j^+)] \pm J \sum_{\langle j,k \rangle} \sigma_j^z \sigma_k^z, \quad (17)$$

where $\delta\Omega \equiv \Omega - \omega_d$ is the detuning.

The Ising-coupling strength J can be designed to be positive (anti-ferromagnetic coupling) or negative (ferromagnetic coupling), depending on the particular physical realization [36]. We consider the special case where the

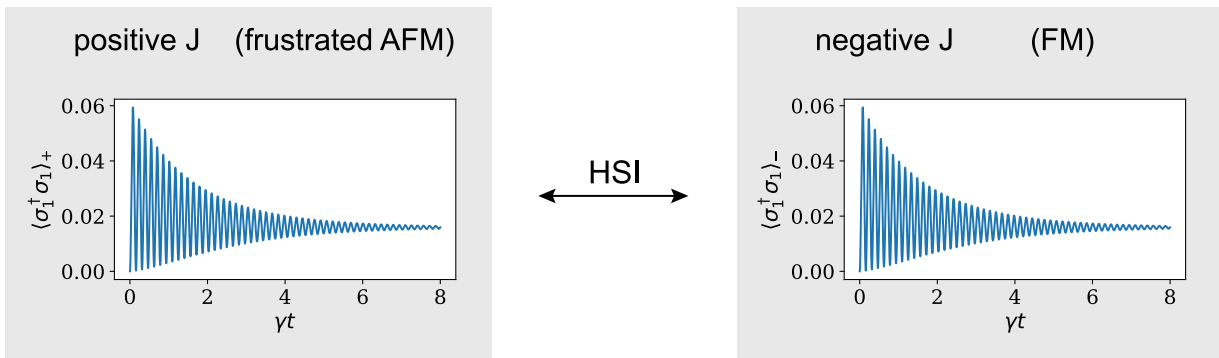


FIG. 2: **Dynamics of spin excitation numbers for a triangular plaquette of Ising-coupled spins subject to driving and dissipation, with antiferromagnetic and ferromagnetic coupling.** The excitation number $\langle \sigma_1^\dagger \sigma_1 \rangle_{\pm}$ is observed to follow the same dynamics for the frustrated (+) and non-frustrated (-) case. (Parameters: $\delta\Omega/\gamma = \pm 1$, $\epsilon/\gamma = 5$ and $J/\gamma = \pm 5$; initial state: all spins in ground state.)

underlying lattice is not bipartite, such as a triangular or Kagome lattice. In this case, ferromagnetic and antiferromagnetic coupling are well known to lead to very different equilibrium physics: while for $\Omega = 0$ the negative- J ground state is a simple ferromagnet, the positive- J case faces geometrical frustration of the antiferromagnetic coupling – a situation of great interest in many-body physics, e.g. in the study of spin glasses [37]. Despite the dramatically different ground-state physics of the geometrically frustrated and non-frustrated lattices, one finds that the HSI mapping (15) establishes a one-to-one correspondence for the out-of-equilibrium dynamics under driving and damping. Similar to \mathbf{a}_j in the harmonic oscillator case, one verifies that the spin lowering operator σ_j^- for pseudospins is invariant under time reversal. Hence, it is straightforward to apply the HSI mapping and obtain

Q_1	<table style="width: 100%; border-collapse: collapse;"> <tr> <td style="padding: 2px;">system parameters</td> <td style="padding: 2px;">$J; \delta\Omega, \epsilon_j$</td> </tr> <tr> <td style="padding: 2px;">damping rate</td> <td style="padding: 2px;">Γ</td> </tr> <tr> <td style="padding: 2px;">density matrix</td> <td style="padding: 2px;">$\rho_1(t)$</td> </tr> <tr> <td style="padding: 2px;">expectation values</td> <td style="padding: 2px;">$\langle A \rangle_1$</td> </tr> </table>	system parameters	$J; \delta\Omega, \epsilon_j$	damping rate	Γ	density matrix	$\rho_1(t)$	expectation values	$\langle A \rangle_1$	$\xleftrightarrow{\text{HSI}}$	<table style="width: 100%; border-collapse: collapse;"> <tr> <td style="padding: 2px;">system parameters</td> <td style="padding: 2px;">$-J; -\delta\Omega, -\epsilon_j$</td> </tr> <tr> <td style="padding: 2px;">damping rate</td> <td style="padding: 2px;">Γ</td> </tr> <tr> <td style="padding: 2px;">density matrix</td> <td style="padding: 2px;">$\rho_2(t) = T\rho_1(t)T^\dagger$</td> </tr> <tr> <td style="padding: 2px;">expectation values</td> <td style="padding: 2px;">$\langle A \rangle_2 = \langle T^\dagger A T \rangle_1^*$</td> </tr> </table>	system parameters	$-J; -\delta\Omega, -\epsilon_j$	damping rate	Γ	density matrix	$\rho_2(t) = T\rho_1(t)T^\dagger$	expectation values	$\langle A \rangle_2 = \langle T^\dagger A T \rangle_1^*$	(18)
system parameters	$J; \delta\Omega, \epsilon_j$																			
damping rate	Γ																			
density matrix	$\rho_1(t)$																			
expectation values	$\langle A \rangle_1$																			
system parameters	$-J; -\delta\Omega, -\epsilon_j$																			
damping rate	Γ																			
density matrix	$\rho_2(t) = T\rho_1(t)T^\dagger$																			
expectation values	$\langle A \rangle_2 = \langle T^\dagger A T \rangle_1^*$																			

where system Q_1 is the frustrated spin lattice, Q_2 the non-frustrated lattice. We can make the Hamiltonian of Q_2 match the one in Q_1 even more closely by eliminating the sign change in the drive strength ϵ_j with a gauge transformation, $\sigma_j^x \rightarrow -\sigma_j^x$ and $\sigma_j^y \rightarrow -\sigma_j^y$ for all sites j . As a result of this, we find a one-to-one correspondence between the frustrated and non-frustrated spin dynamics and steady state in a driven-dissipative Ising lattice. (The only parameter to be adjusted is the drive-frequency detuning $\delta\Omega$.)

For numerical confirmation of this result we have simulated the dynamics for a triangular plaquette of three spins, see Fig. 2. (In this simulation, only one of the three sites is driven and the spin excitation number on that particular site is monitored.) We find the expected, but non-intuitive, result that the nonequilibrium dynamics are indeed identical in the frustrated and the non-frustrated case.

V. CONCLUSION

We have proven and illustrated the use of a mapping that establishes a one-to-one correspondence between nonequilibrium dynamics of one Markovian open quantum system and a second such system whose Hamiltonian carries the opposite sign. This mapping relies on the time-reversal invariant of the system Hamiltonian, and makes the remarkable prediction that nonequilibrium dynamics of different systems can be essentially identical despite the fact that their equilibrium physics is extremely different. We demonstrated this Hamiltonian sign inversion mapping for two concrete examples: the driven-dissipative Bose-Hubbard dimer for attractive vs. repulsive onsite interaction, and a driven-dissipative Ising spin lattice model with and without geometrical frustration.

The HSI mapping is widely applicable to many interesting driven-dissipative quantum models realizable by ultracold atoms and circuit-QED architecture, and allows important conclusions. For instance, from the HSI mapping we can immediately infer that the symmetry-breaking state predicted for the driven-dissipative *repulsive* Bose-Hubbard dimer [22] must also occur for the case of an *attractive* dimer. Establishing such mappings will not only facilitate a better understanding of the relation between broken symmetry and the nature of nonlinearities, but also motivate

new experiments probing nonequilibrium many-body phenomena. We believe that the HSI mapping will serve as a valuable tool in the study of nonequilibrium dynamics, steady-state properties, and dissipative phase transitions in open quantum systems.

Acknowledgments

We acknowledge valuable discussions with Peter Groszkowski, Mattias Fitzpatrick, Neereja Sundaresan, A. A. Houck and M. I. Dykman. This research was supported in part by the NSF under Grant No. PHY-1055993 (A.C.Y.L. and J.K.).

Appendix A: Equations of motion of the driven-dissipative Bose-Hubbard dimer model

In this appendix, we demonstrate that expectation values of the general operators $A_{r,s}^{p,q} = (\mathbf{a}_1^\dagger)^p (\mathbf{a}_2^\dagger)^q \mathbf{a}_1^r \mathbf{a}_2^s$ indeed obey the relation

$$\langle A_{r,s}^{p,q}(-\mathbf{p}) \rangle_- = \langle A_{r,s}^{p,q}(\mathbf{p}) \rangle_+^*, \quad (\text{A1})$$

see Eq. (8) in the main text. We abbreviate the positive- U expectation value by $A_{r,s}^{p,q} = \langle A_{r,s}^{p,q}(\mathbf{p}) \rangle_+$ and deduce the corresponding equation of motion from the master equation (2). We find:

$$\begin{aligned} i \frac{dA_{r,s}^{p,q}}{dt} = & \left[(\delta\omega - U)(r + s - p - q) + U(r^2 + s^2 - p^2 - q^2) - \frac{i\gamma}{2}(p + q + r + s) \right] A_{r,s}^{p,q} + 2U \left[(r - p)A_{r+1,s}^{p+1,q} + (s - q)A_{r,s+1}^{p,q+1} \right] \\ & + J \left[rA_{r-1,s+1}^{p,q} + sA_{r+1,s-1}^{p,q} - pA_{r,s}^{p-1,q+1} - qA_{r,s}^{p+1,q-1} \right] + \epsilon \left[rA_{r-1,s}^{p,q} - pA_{r,s}^{p-1,q} \right]. \end{aligned} \quad (\text{A2})$$

By complex conjugation of this equation, we obtain

$$\begin{aligned} i \frac{dA_{r,s}^{p,q*}}{dt} = & \left[(-\delta\omega + U)(r + s - p - q) - U(r^2 + s^2 - p^2 - q^2) - \frac{i\gamma}{2}(p + q + r + s) \right] A_{r,s}^{p,q*} - 2U \left[(r - p)A_{r+1,s}^{p+1,q*} + (s - q)A_{r,s+1}^{p,q+1*} \right] \\ & - J \left[rA_{r-1,s+1}^{p,q*} + sA_{r+1,s-1}^{p,q*} - pA_{r,s}^{p-1,q+1*} - qA_{r,s}^{p+1,q-1*} \right] - \epsilon \left[rA_{r-1,s}^{p,q*} - pA_{r,s}^{p-1,q*} \right]. \end{aligned} \quad (\text{A3})$$

Comparison of the latter equation with the equation of motion for the corresponding negative- U expectation value confirms the proposed relation (A1).

-
- [1] T. Grujic, S. R. Clark, D. Jaksch, and D. G. Angelakis, *Repulsively induced photon superbunching in driven resonator arrays*, *Phys. Rev. A* **87**, 053846 (2013).
 - [2] K. D. B. Higgins, S. C. Benjamin, T. M. Stace, G. J. Milburn, B. W. Lovett, and E. M. Gauger, *Superabsorption of light via quantum engineering*, *Nat. Commun.* **5**, 4705 (2014).
 - [3] J. Raftery, D. Sadri, S. Schmidt, H. E. Türeci, and A. A. Houck, *Observation of a dissipation-induced classical to quantum transition*, *Phys. Rev. X* **4**, 031043 (2014).
 - [4] J. Klinder, H. Keßler, M. Wolke, L. Mathey, and A. Hemmerich, *Dynamical phase transition in the open Dicke model*, *Proc. Natl. Acad. Sci. U.S.A.* **112**, 3290 (2015).
 - [5] P. Hamel, S. Haddadi, F. Raineri, P. Monnier, G. Beaudoin, I. Sagnes, A. Levenson, and A. M. Yacomotti, *Spontaneous mirror-symmetry breaking in coupled photonic-crystal nanolasers*, *Nat. Photon.* **9**, 311 (2015).
 - [6] T. E. Lee, H. Häffner, and M. C. Cross, *Collective quantum jumps of Rydberg atoms*, *Phys. Rev. Lett.* **108**, 023602 (2012).
 - [7] E. M. Kessler, G. Giedke, A. Imamoglu, S. F. Yelin, M. D. Lukin, and J. I. Cirac, *Dissipative phase transition in a central spin system*, *Phys. Rev. A* **86**, 012116 (2012).
 - [8] H. J. Carmichael, *Breakdown of photon blockade: A dissipative quantum phase transition in zero dimensions*, *Phys. Rev. X* **5**, 031028 (2015).
 - [9] W. Casteels, R. Fazio, and C. Ciuti, *Critical dynamical properties of a first-order dissipative phase transition*, *Phys. Rev. A* **95**, 012128 (2017).

- [10] J. M. Fink, A. Dombi, A. Vukics, A. Wallraff, and P. Domokos, *Observation of the photon-blockade breakdown phase transition*, *Phys. Rev. X* **7**, 011012 (2017).
- [11] M. Fitzpatrick, N. M. Sundaresan, A. C. Y. Li, J. Koch, and A. A. Houck, *Observation of a dissipative phase transition in a one-dimensional circuit qed lattice*, *Phys. Rev. X* **7**, 011016 (2017).
- [12] B. Kraus, H. P. Büchler, S. Diehl, A. Kantian, A. Micheli, and P. Zoller, *Preparation of entangled states by quantum Markov processes*, *Phys. Rev. A* **78**, 042307 (2008).
- [13] R. Sweke, I. Sinayskiy, and F. Petruccione, *Dissipative preparation of generalized Bell states*, *J. Phys. B* **46**, 104004 (2013).
- [14] F. Reiter, L. Tornberg, G. Johansson, and A. S. Sørensen, *Steady-state entanglement of two superconducting qubits engineered by dissipation*, *Phys. Rev. A* **88**, 032317 (2013).
- [15] A. Kronwald, F. Marquardt, and A. A. Clerk, *Dissipative optomechanical squeezing of light*, *New J. Phys.* **16**, 063058 (2014).
- [16] C. Aron, M. Kulkarni, and H. E. Türeci, *Steady-state entanglement of spatially separated qubits via quantum bath engineering*, *Phys. Rev. A* **90**, 062305 (2014).
- [17] M. E. Kimchi-Schwartz, L. Martin, E. Flurin, C. Aron, M. Kulkarni, H. E. Tureci, and I. Siddiqi, *Stabilizing entanglement via symmetry-selective bath engineering in superconducting qubits*, *Phys. Rev. Lett.* **116**, 240503 (2016).
- [18] S. Diehl, A. Micheli, A. Kantian, B. Kraus, H. Büchler, and P. Zoller, *Quantum states and phases in driven open quantum systems with cold atoms*, *Nature Phys.* **4**, 878 (2008).
- [19] T. Schulte-Herbrüggen, A. Spörl, N. Khaneja, and S. Glaser, *Optimal control for generating quantum gates in open dissipative systems*, *J. Phys. B* **44**, 154013 (2011).
- [20] N. Oelkers and J. Links, *Ground-state properties of the attractive one-dimensional Bose-Hubbard model*, *Phys. Rev. B* **75**, 115119 (2007).
- [21] E.-M. Graefe, H. J. Korsch, and M. P. Strzys, *Bose-Hubbard dimers, Vivianis windows and pendulum dynamics*, *J. Phys. A* **47**, 085304 (2014).
- [22] B. Cao, K. W. Mahmud, and M. Hafezi, *Two coupled nonlinear cavities in a driven-dissipative environment*, *Phys. Rev. A* **94**, 063805 (2016).
- [23] W. Casteels and C. Ciuti, *Quantum entanglement in the spatial-symmetry-breaking phase transition of a driven-dissipative Bose-Hubbard dimer*, *Phys. Rev. A* **95**, 013812 (2017).
- [24] W. Casteels and M. Wouters, *Optically bistable driven-dissipative Bose-Hubbard dimer: Gutzwiller approaches and entanglement*, *Phys. Rev. A* **95**, 043833 (2017).
- [25] H. Breuer and F. Petruccione, *The Theory Of Open Quantum Systems* (Oxford University Press, 2002).
- [26] K. Lendi, *N-level systems and applications to spectroscopy*, in *Quantum dynamical semigroups and applications* (Springer, 2007).
- [27] L. S. Bishop, J. M. Chow, J. Koch, A. A. Houck, M. H. Devoret, E. Thuneberg, S. M. Girvin, and R. J. Schoelkopf, *Nonlinear response of the vacuum Rabi resonance*, *Nature Phys.* **5**, 105 (2009).
- [28] M. I. Dykman, *Critical exponents in metastable decay via quantum activation*, *Phys. Rev. E* **75**, 011101 (2007).
- [29] E. Wigner, *Group Theory and Its Application to the Quantum Mechanics of Atomic Spectra* (Academic Press, 1959) pp. 325–348.
- [30] V. Bargmann, *Note on Wigner's theorem on symmetry operations*, *J. Math. Phys.* **5**, 862 (1964).
- [31] T. Prosen and M. Žnidarič, *Long-range order in nonequilibrium interacting quantum spin chains*, *Phys. Rev. Lett.* **105**, 060603 (2010).
- [32] T. E. Lee, H. Häffner, and M. C. Cross, *Antiferromagnetic phase transition in a nonequilibrium lattice of Rydberg atoms*, *Phys. Rev. A* **84**, 031402 (2011).
- [33] Z. Cai and T. Barthel, *Algebraic versus exponential decoherence in dissipative many-particle systems*, *Phys. Rev. Lett.* **111**, 150403 (2013).
- [34] H. Schwager, J. I. Cirac, and G. Giedke, *Dissipative spin chains: Implementation with cold atoms and steady-state properties*, *Phys. Rev. A* **87**, 022110 (2013).
- [35] F. Nissen, S. , M. Biondi, G. Blatter, H. E. Türeci, and J. Keeling, *Nonequilibrium dynamics of coupled qubit-cavity arrays*, *Phys. Rev. Lett.* **108**, 233603 (2012).
- [36] O. Viehmann, J. von Delft, and F. Marquardt, *Observing the nonequilibrium dynamics of the quantum transverse-field Ising chain in circuit QED*, *Phys. Rev. Lett.* **110**, 030601 (2013).
- [37] A. P. Ramirez, *Strongly geometrically frustrated magnets*, *Annu. Rev. Mater. Sci.* **24**, 453 (1994).
- [38] J. Koch, T. M. Yu, J. Gambetta, A. A. Houck, D. I. Schuster, J. Majer, A. Blais, M. H. Devoret, S. M. Girvin, and R. J. Schoelkopf, *Charge-insensitive qubit design derived from the Cooper pair box*, *Phys. Rev. A* **76**, 042319 (2007).
- [39] For example when using the attractive Bose-Hubbard model as an approximation of a transmon qubit, excitations with energies above the maximum of the cosine potential will break the Bose-Hubbard approximation [38]. In that case, a perturbative treatment of the potential is not appropriate.
- [40] The annihilation operator is defined by $\mathbf{a} = \frac{1}{\sqrt{2}}(\frac{\mathbf{x}}{x_0} + i\frac{\mathbf{p}}{p_0})$ where \mathbf{x} is a generalized position and \mathbf{p} a generalized momentum operator; x_0, p_0 are constants. From $\mathbf{T}\mathbf{x}\mathbf{T}^\dagger = \mathbf{x}$, $\mathbf{T}\mathbf{p}\mathbf{T}^\dagger = -\mathbf{p}$, and anti-linearity of \mathbf{T} follows the time-reversal invariance of \mathbf{a}_j .